Steady-State Temperature Profiles in a UMLRR Fuel Channel

Introduction

When modeling some phenomena of interest, one should always start with a relatively simple model so that you can obtain a good understanding of the basic behavior of the system. Once you have a good appreciation for the basic theory and a feel for the qualitative and quantitative behavior of the system, then you can add additional complexities, as needed, to model the real phenomena of interest. This documentation follows this philosophy with the development of a relatively simple model for the energy removal process within a plate-type fuel channel. The specific case of interest involves a single fuel plate and associated coolant channel within the UMass-Lowell Research Reactor (UMLRR). The goal is to compute and plot the axial temperature profiles within the coolant channel, clad, and fuel plate for the average or hot plate within the reactor. In addition, this report also addresses the modeling of both the forced and natural convection cases.

We start with a specific representation of a plate-type fuel assembly that uses a variety of assumptions to simplify the analysis to the point that analytical solutions can be obtained. The focus here will be on a single plate and channel configuration (a unit cell analysis), with the assumption that this same configuration is repeated many times within a single assembly, which is then repeated multiple times to make up the actual UMLRR core.

We break the discussion/analyses in this set of notes into several major sections:

- Background description of the UMLRR core and the physical fuel element arrangement.
- Development of the steady state heat conduction equation.
- Heat transfer in the solid fuel plate and cladding (radial heat transfer).
- Heat transfer into the coolant channel (energy flows both radially and axially).
- Description of the axial power profile in a typical fuel plate.
- Calculation of the heat transfer coefficient in both forced and natural convection flows.
- Treatment of the water properties versus temperature.
- Computation of the mass flow rate in natural convection flows.
- Nominal UMLRR operational and design data.
- Typical results for the UMLRR.

Note that all the analyses done here assume steady state conditions.

Background Description of a UMLRR Fuel Element

In this work we consider a series of heated, parallel, vertical, rectangular channels, such as the coolant channels within a standard fuel element in the UMass-Lowell research reactor (UMLRR), as illustrated in Figs. 1-4. These figures show a 3-D view of the basic fuel assembly geometry containing a series of fuel plates and coolant channels, a view of the reactor core box and the 9x7 grid structure that holds the fuel elements and a variety of other core components, the specific arrangement of the current core configuration showing the placement of 19 full and 2

partial fuel elements within the grid (M-2-5 configuration), and a CAD drawing showing the top view and dimension details of a typical fuel assembly. The reactor core is located in a large open pool containing about 76000 gallons of water. The top of the fuel region is about 25 feet below the surface of the pool.

The UMLRR is licensed to operate at a maximum thermal power of 1 MW in forced convection mode, where the coolant flow is downward through the core with a total flow rate of about 1650 gpm. The facility can also operate in natural convection mode with a maximum licensed power level of 100 kW. In this case, the density differences in the fuel channels and the surrounding pool water create a buoyancy force that causes the coolant to flow upward in the channels. Our interest in this set of notes is to develop a mathematical model for determining the steady state axial profile of the coolant, plate surface, fuel surface, and fuel centerline temperatures under a variety of typical conditions that can exist in the reactor (including both forced and natural convection conditions).

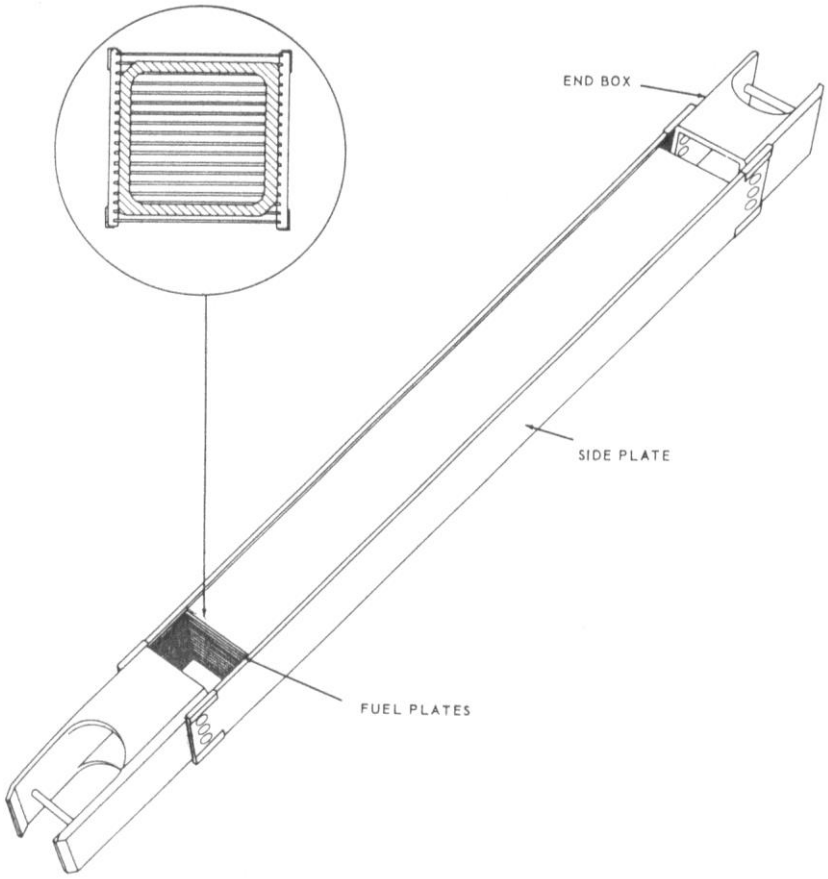

Fig. 1 Isometric view of a typical fuel assembly.

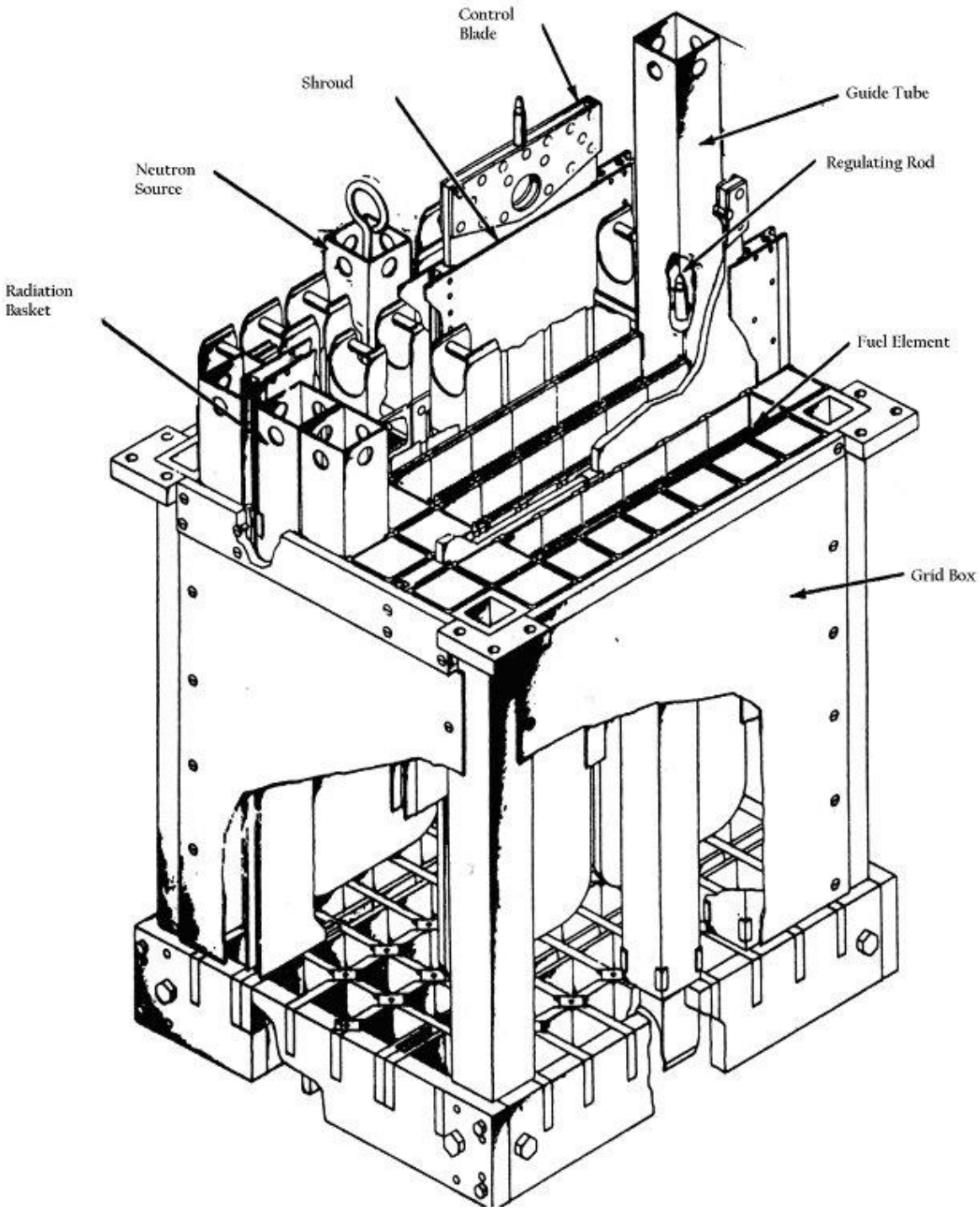

Fig. 2 Core box geometry showing placement of various components within the UMLRR.

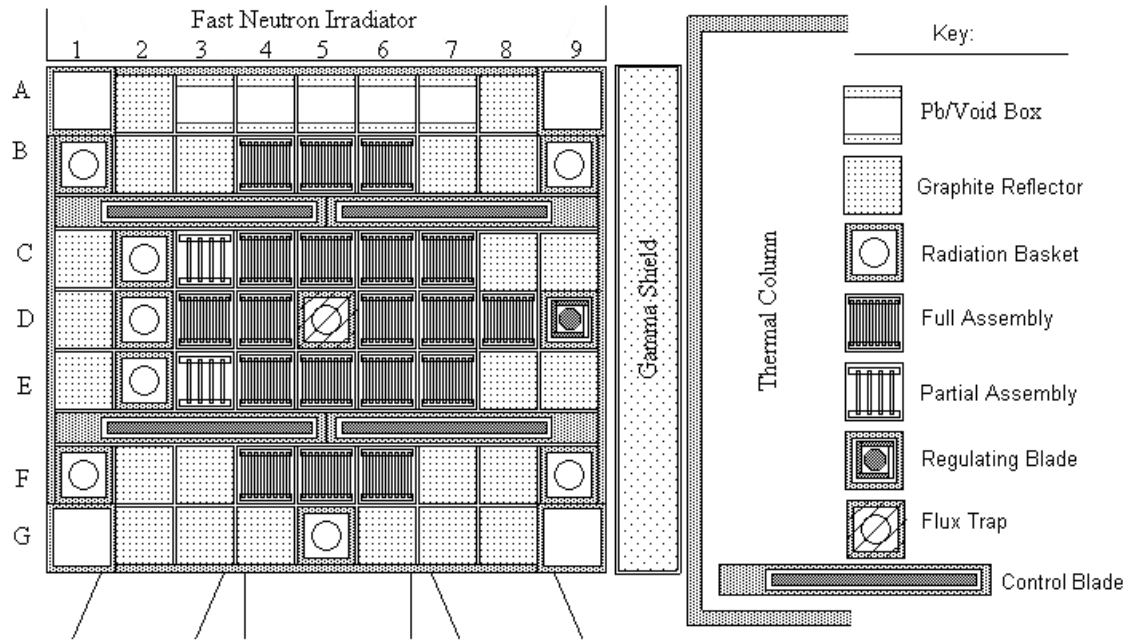

Fig. 3 Core layout showing placement of the fuel assemblies within the UMLRR grid.

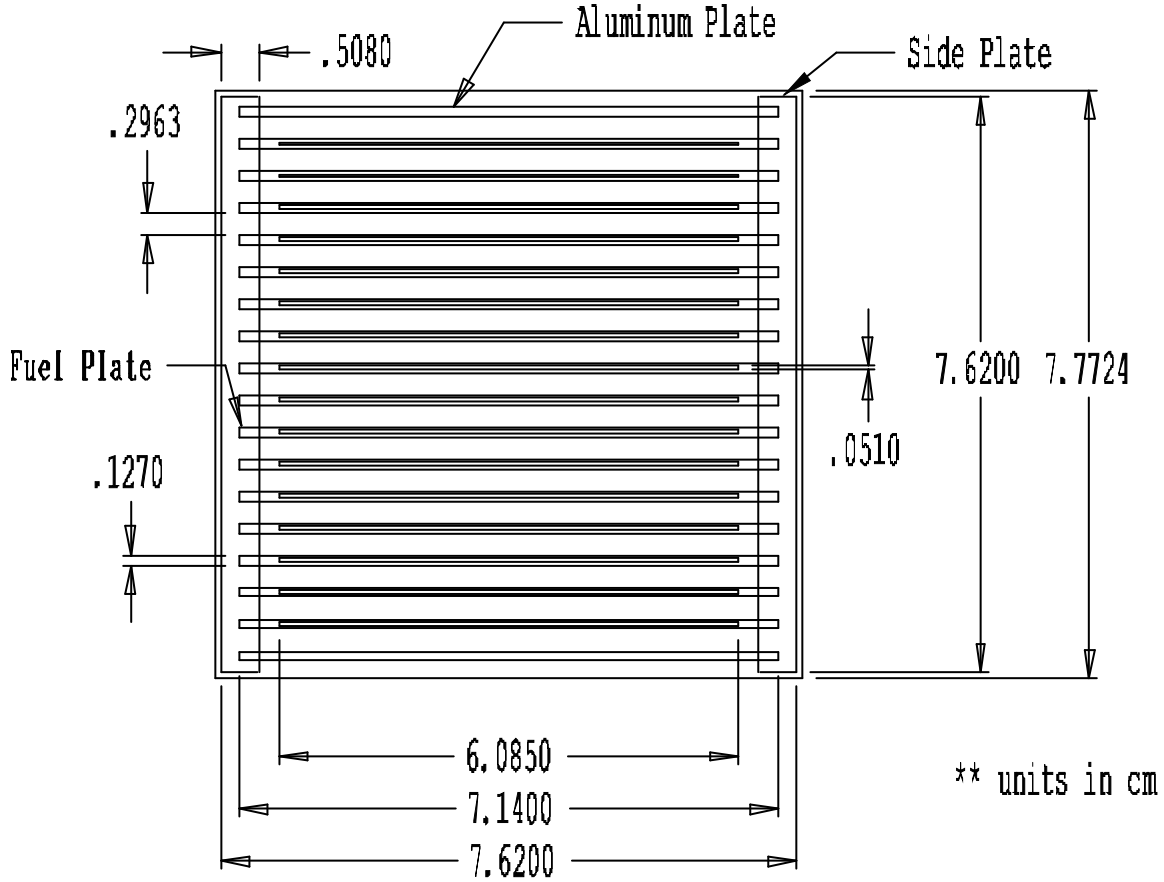

Fig. 4 Standard fuel assembly geometry (top view) with 16 fuel plates per assembly.

Conduction Heat Transfer in a Solid Control Volume

We start with a general development of the heat conduction equation. At steady state, the rate of energy production in volume V minus the net rate of energy flow out of V must balance, or

$$\int_V q'''\,d\vec{r} - \int_A \vec{q}''\bullet\hat{n}\,dA = 0 \qquad (1)$$

where q''' = volumetric internal energy production rate (W/m^3)

$d\vec{r}$ = differential volume (m^3)

$\vec{q}''$ = heat flux vector (W/m^2)

$\hat{n}$ = outward pointing normal vector (unit vector perpendicular to the surface)

$dA = w\,dz$ = differential area, with w representing the width of the fuel region.

But the Divergence Theorem allows us to convert the area integral in eqn. (1) into a volume integral,

$$\int_A \vec{q}''\bullet\hat{n}dA = \int_V \vec{\nabla}\bullet\vec{q}''\,d\vec{r} \qquad (2)$$

Therefore, eqn. (1) becomes

$$\int_V q'''\,d\vec{r} - \int_V \vec{\nabla}\bullet\vec{q}''\,d\vec{r} = 0 \qquad (3)$$

And, since these are integrated over the same arbitrary volume, we can write a differential balance (per unit volume) as

$$-\vec{\nabla}\bullet\vec{q}'' + q''' = 0 \qquad (4)$$

But Fourier's Law of heat conduction gives

$$\vec{q}'' = -k\vec{\nabla}T \qquad (5)$$

Therefore the steady state heat conduction equation becomes

$$\vec{\nabla}\bullet k\vec{\nabla}T + q''' = 0 \qquad (6)$$

If k is constant, then this becomes

$$\nabla^2 T + q'''/k = 0 \qquad (7)$$

where k is the thermal conductivity of the material (W/m-°C)

Note that the units for the temperature gradient are $\vec{\nabla}T \rightarrow {}^{o}C/m$, $\nabla^2 T \rightarrow {}^{o}C/m^2$ and, for q'''/k, we have

$$\frac{q'''}{k} \rightarrow \frac{W/m^3}{W/m - {}^{o}C} \rightarrow \frac{{}^{o}C}{m^2}$$

which, as expected, are identical to $\nabla^2 T$ [via eqn. (7)].

In preliminary analysis, we often let k be constant and use eqn. (7) for the geometry of interest. In later, more detailed analysis, k is allowed to be space and temperature dependent (which leads to a nonlinear relationship). This situation is usually not treated analytically -- instead numerical methods are applied.

Thus, for our simple preliminary analysis here, we will assume that k is an appropriately averaged constant for each solid material of interest.

Heat Transfer in the Solid Fuel Plate

The basic configuration of interest in this development is illustrated in Fig. 5 where the specific notation is defined as follows:

a = half thickness of fuel, b = clad thickness, c = half thickness of water channel

T_m = fuel centerline temperature, T_s = fuel surface temperature

T_c = clad surface temperature, T_b = bulk coolant temperature

where all the temperatures are functions of the axial location, z [i.e. all $T_j \rightarrow T_j(z)$].

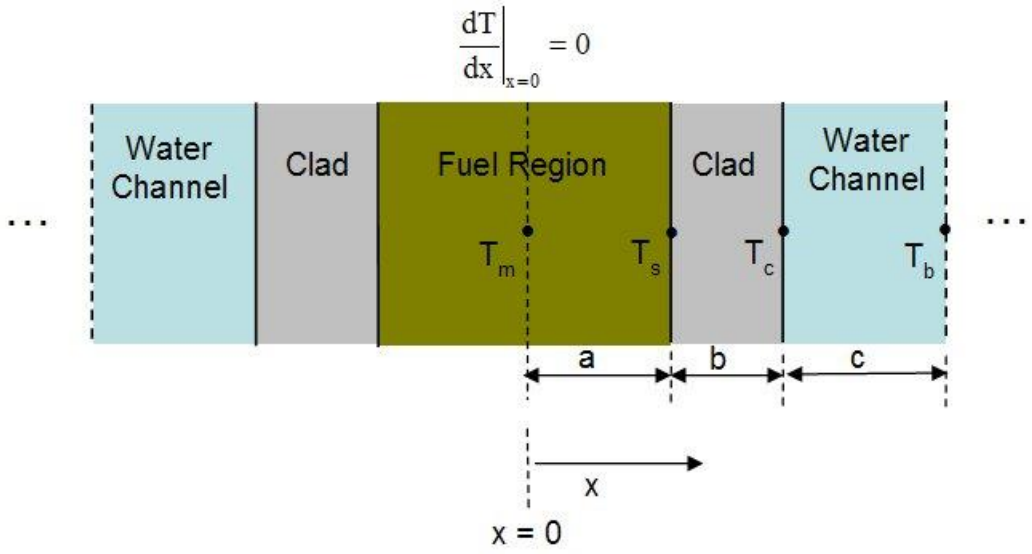

Fig. 5 Sketch of 1-D fuel plate, clad, and coolant geometry.

The assumptions inherent in the subsequent modeling are listed below:

1. All energy is transported radially through the fuel, through the clad, to the coolant. Since the coolant flow is in the axial direction, everything will vary with axial location z. Also note that the internal energy generation term, q''', varies axially. However, at each axial layer, z, we are assuming that all the energy flows in the radial direction. This allows us to use the 1-D version of eqns. (6) and (7) in the formal analysis.
2. Assume k = constant -- therefore we will use eqn. (7) for the heat transfer analysis.

3. Assume q‴ is constant at each axial layer, that is q‴(x,y,z) = q‴(z) = constant at each z. Also all the plates have the same q‴ for the ***average plate*** analysis and this value is simply multiplied by the radial peaking factor for the ***hot plate*** analysis.

4. Assume symmetry at x = 0, or $\left.\frac{dT}{dx}\right|_{x=0} = 0$

Note that all these assumptions are very reasonable for the problem of interest here. Assumption #4 is not strictly valid for fuel plates near the end of the fuel assembly, but it is a very good approximation for the plates in the interior of the element.

Fuel Region (at any axial location z)

Equation (7) specialized to the case of 1-D Cartesian geometry can be written as

$$\frac{d^2T}{dx^2} + \frac{q'''}{k_f} = 0 \tag{8}$$

where k_f is the thermal conductivity of the fuel. Integrating this expression gives

$$\frac{dT}{dx} = -\frac{q'''}{k_f}x + C_1 \tag{9}$$

and a second integration gives

$$T(x) = -\frac{q'''}{2k_f}x^2 + C_1 x + C_2 \tag{10}$$

Now applying the symmetry boundary condition at x = 0, eqn. (9) gives

$$\left.\frac{dT}{dx}\right|_{x=0} = 0 = C_1$$

At x = a (the fuel meat half thickness), the fuel surface temperature is denoted as T_s, as shown in Fig. 5. Thus, evaluating eqn. (10) at x = a with $C_1 = 0$ gives

$$T_s = -\frac{q'''}{2k_f}a^2 + C_2 \qquad \text{or} \qquad C_2 = T_s + \frac{q'''}{2k_f}a^2$$

which yields a continuous expression for the radial temperature distribution within the fuel meat,

$$T(x) = T_s + \frac{q'''}{2k_f}(a^2 - x^2) \tag{11}$$

For convenience we also denote the fuel centerline temperature as $T(0) = T_m$ (since, in a symmetric arrangement, the maximum temperature will occur at the center of the plate). With this notation, eqn. (11) reduces to

$$T_m - T_s = \frac{q'''}{2k_f}a^2 \tag{12}$$

As you probably already know, for 1-D heat transfer analyses, it is often convenient to use an electrical analogy to help interpret and visualize the various energy flow rates. In electrical

circuits, the current, I, times the resistance, R, is equal to the driving potential or voltage, V, or V = IR -- this is referred to as ***Ohm's Law***. Within this context we can think of the temperature difference, $T_m - T_s$, as the driving potential for heat flow in the fuel region, and define q″ as the heat flux or energy flow rate per unit area out of the fuel region (right face). The heat flux in our example is analogous to the current (i.e. the quantity that flows) in an electrical circuit. Thus, we can write Ohm's Law for 1-D heat transfer in 1-D Cartesian geometry as

$$I = \frac{V}{R} \qquad \text{or} \qquad q'' = \frac{\Delta T}{R_{th}} = \frac{T_m - T_s}{R_f} \tag{13}$$

where R_{th} is a generic thermal resistance (i.e. the resistance to energy transport in the region between the given ΔT) and R_f is the specific thermal resistance for the fuel material.

For Cartesian geometry and steady state conditions the same heat flux given in eqn. (13) must also pass through the clad and into the coolant (all the energy generated in the fuel is removed by the coolant). Based on this observation, we can also extend this electrical analogy to the clad and coolant regions (refer to Fig. 5 for the pertinent notation), or

$$q'' = \frac{\Delta T}{R_{th}} = \frac{T_m - T_s}{R_f} = \frac{T_s - T_c}{R_c} = \frac{T_c - T_b}{R_b} \tag{14}$$

where R_c is the thermal resistance to heat transfer in the clad region and R_b is the resistance to convection heat transfer from the clad surface to the bulk fluid.

Equation (14) is extremely important. To see this, assume for the moment that we know $T_b(z)$ and the three thermal resistances, R_f, R_c, and R_b. With these quantities and eqn. (14), we can write explicit expressions for $T_c(z)$, $T_s(z)$, and $T_m(z)$, as follows:

$$T_c(z) = T_b(z) + R_b q''(z) \tag{15a}$$

$$T_s(z) = T_c(z) + R_c q''(z) \qquad \text{or} \qquad T_s(z) = T_b(z) + \left(R_c + R_b\right) q''(z) \tag{15b}$$

$$T_m(z) = T_s(z) + R_f q''(z) \qquad \text{or} \qquad T_m(z) = T_b(z) + \left(R_f + R_c + R_b\right) q''(z) \tag{15c}$$

where q″(z) can be written in terms of the volumetric heat generation rate, q‴(z) , as

$$q''(z) = a\, q'''(z) \tag{16}$$

with the variable 'a' representing the half width of the fuel meat (i.e. a·q‴(z) is the energy transfer rate per unit area out of the fuel at axial location z).

For a given problem, the geometry parameters and the axial heat generation rate profile must be known [see below for further discussion of q‴(z)]. Thus, evaluation of eqns. (15a) – (15c) reduces to actually determining explicit expressions for the three thermal resistances and the axial profile of the bulk coolant temperature, $T_b(z)$.

For R_f we can compare eqns. (12) and (13) to immediately give

$$\frac{2k_f}{a}\left(T_m - T_s\right) = q'''a = q'' \qquad \text{or} \qquad R_f = \frac{a}{2k_f} \tag{17}$$

where R_f is the equivalent thermal resistance of the fuel.

Clad Region

For the thermal resistance in the clad region, we again solve the heat conduction equation, but this time q‴ = 0 since we assume negligible energy deposition directly in the clad. Therefore, the heat conduction equation in 1-D Cartesian geometry is simply

$$\frac{d^2T}{dx^2} = 0 \tag{18}$$

and integrating twice yields the general solution

$$T(x) = C_1x + C_2 \tag{19}$$

Now, applying the appropriate boundary conditions at x = a and x = a+b gives

$$T(a) = T_s = C_1a + C_2 \qquad \text{and} \qquad T(a+b) = T_c = C_1(a+b) + C_2 \tag{20}$$

Subtracting these two expressions gives

$$T_c - T_s = C_1b \qquad \text{or} \qquad C_1 = \frac{T_c - T_s}{b} \tag{21}$$

and substituting the expression for C_1 into the first expression in eqn. (20) gives

$$T_s = \frac{(T_c - T_{s)}}{b}a + C_2 \qquad \text{or} \qquad C_2 = T_s - \frac{(T_c - T_s)}{b}a \tag{22}$$

Finally, putting these into the general solution and simplifying gives

$$T(x) = \frac{T_c - T_s}{b}x + T_s - \frac{(T_c - T_s)}{b}a$$

or

$$T(x) = T_s + \frac{T_c - T_s}{b}(x - a) \qquad \text{for } a \le x \le a + b \tag{23}$$

Now, to use the electrical analogy again, we know that the heat flux leaving the right face (at x = a+b) is given by Fourier's law,

$$q'' = -k_c \left.\frac{dT}{dx}\right|_{x=a+b} = -k_c \frac{T_c - T_s}{b} = k_c \frac{T_s - T_c}{b} \tag{24}$$

where k_c is the clad thermal conductivity and b is the thickness of the clad.

Finally, comparing this to the definition of the clad thermal resistance, R_c, given by eqn. (14), we see that R_c can be written explicitly as

$$R_c = \frac{b}{k_c} \tag{25}$$

Heat Transfer to the Coolant Channel

To address the transfer of energy from the fuel to the coolant, let's first isolate a single coolant channel with dimensions D, W, and H to specify the channel geometry as shown in Fig. 6 (note that the depth D in Fig. 6 is equivalent to 2c from Fig. 5, where c was defined as the half thickness of the channel, and that H refers to the active fuel height). For long, thin fuel elements, axial conduction is negligible compared to the radial flow of energy from the fuel plate to the coolant channel. Thus, in each axial increment, all the energy generated in the fuel is transferred to the coolant via convection heat transfer.

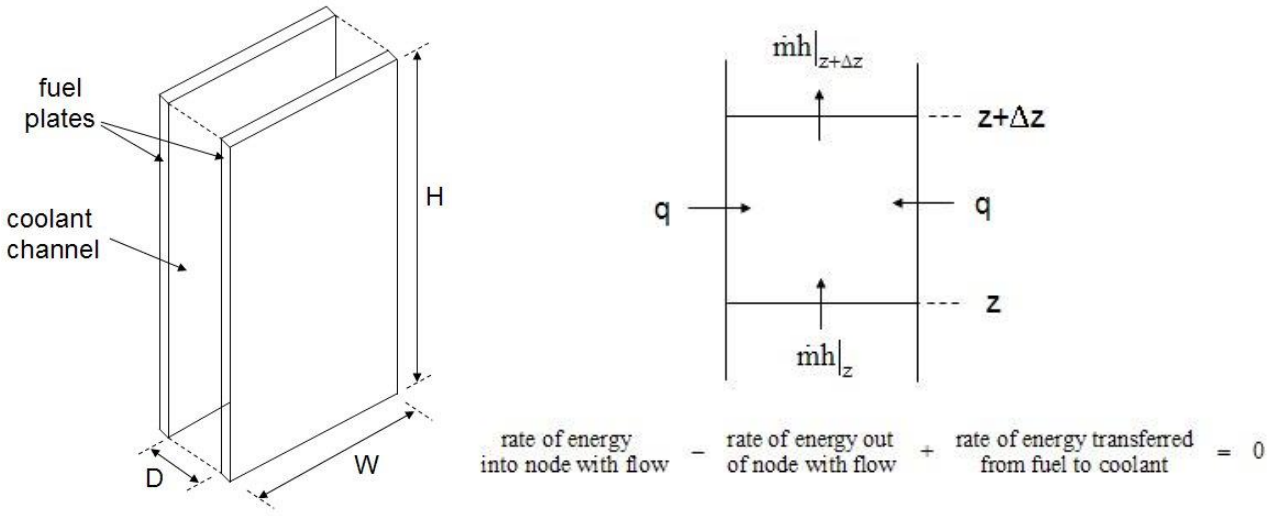

Fig. 6 Geometry for a single coolant channel and balance on coolant node of height Δz.

A steady state energy balance on a fluid node can be given as shown on the right side of Fig. 6. This balance can be written mathematically as

$$\dot{m}h\big|_z - \dot{m}h\big|_{z+\Delta z} + q''(z)2W\Delta z = 0 \qquad (26)$$

where $\dot{m}$ is the mass flow rate in a single coolant channel

h is the fluid enthalpy per unit mass

and $q = q''\cdot 2W\Delta z$ is the heat transfer from the fuel to the coolant within axial height Δz

Now, dividing eqn. (26) by Δz and taking the limit as $\Delta z \to 0$ gives

$$\frac{dh(z)}{dz} = \frac{2W}{\dot{m}} q''(z) \qquad (27)$$

However, for single phase systems, we can relate the enthalpy change to a change in temperature via an average specific heat (i.e. $dh = c_p dT$), giving

$$\frac{dT_b(z)}{dz} = \frac{2W}{\dot{m}c_p} q''(z) \qquad \text{with} \quad T_b(0) = T_{in} \qquad (28)$$

where $T_b(z)$ is the bulk fluid temperature at axial height z and T_{in} is the inlet coolant temperature from the pool. If the channel mass flow rate, $\dot{m}$, and the axial profile of the heat flux, $q''(z)$, are known, then this simple 1st order IVP can be solved for the desired temperature profile, $T_b(z)$.

Note that once the coolant temperature, $T_b(z)$, has been determined, one can also find the clad surface temperature [which we defined previously as $T_c(z)$] from Newton's Law of Cooling,

$$q''(z) = h\left(T_c(z) - T_b(z)\right) \tag{29}$$

where h is the heat transfer coefficient. (Note: In the above discussion h was used for enthalpy -- but in eqn. (28) we wrote this variable in terms of the temperature -- so now we can use h to refer to the proportionality constant in Newton's Law of Cooling.) Solving eqn. (29) for the clad surface temperature gives

$$T_c(z) = T_b(z) + \frac{1}{h} q''(z) \tag{30}$$

and, comparing this to eqn. (15a), we see that the resistance to energy transfer between the clad and bulk fluid is simply, $R_b = 1/h$.

Axial Profile of the Surface Heat Flux

The energy generation in the fuel results from the nuclear fission process. In steady state, all the energy produced within the fuel plate must leave the plate via convection heat transfer on its surfaces. If there are N_{fp} fuel plates in the core and the total power level is denoted as P_{tot}, then the power produced by the average or typical fuel plate is simply $P_{plate} = P_{tot}/N_{fp}$. Now, the average heat flux on the surface of the plates is simply the plate power divided by the heat transfer surface area. Thus, using the geometry notation from Fig. 6, we have

$$q''_{ave} = \frac{P_{plate}}{2WH} = \frac{P_{tot}}{2N_{fp}WH} \tag{31}$$

In a typical UMLRR fuel plate, the spatial distribution of the fission rate is nearly constant in the x and y directions for any given z location, and its axial shape is roughly sinusoidal in nature (it is slightly bottom-peaked but, for simplicity, we will assume axial symmetry here). In the ideal symmetric case, we can write this axial dependence as a chopped sinusoid,

$$q''(z) = q''_{max} \sin\left(\frac{\pi(z+\delta)}{H_e}\right) \tag{32}$$

where q''_{max} = peak heat flux (W/m^2) within an average plate (this occurs at core center -- at z = H/2 -- for a symmetric axial profile)

H_e = effective neutronic height of the core (m)

δ = reflector savings (m) which is defined through the relationship between H and H_e, where $H_e = H + 2\delta$)

The peak heat flux, q''_{max}, is related to the plate power [and q''_{ave} via eqn. (31)] as follows:

$$P_{plate} = 2\int_0^W \int_0^H q"_{max} \sin\left(\frac{\pi(z+\delta)}{H_e}\right) dydz = 2Wq"_{max} \int_0^H \sin\left(\frac{\pi(z+\delta)}{H_e}\right) dz$$

or,

$$q"_{max} = \frac{P_{plate}}{2W\int_0^H \sin\left(\frac{\pi(z+\delta)}{H_e}\right) dz} \tag{33}$$

Given the necessary core design and operational data, eqn. (33) can be evaluated to find a numerical value for $q"_{max}$ for use in eqn. (32) to describe the axial profile of the heat flux along the plate surface. This expression, in turn, can be used in eqns. (28) and (30) to define $T_b(z)$ and $T_c(z)$, respectively.

Performing the operation indicated in eqn. (33) gives

$$q"_{max} = \frac{\pi P_{plate}}{2WH_e} \frac{1}{\cos\left(\frac{\pi\delta}{H_e}\right) - \cos\left(\frac{\pi(H+\delta)}{H_e}\right)} \tag{34}$$

Now, putting eqns. (32) and (34) into eqn. (28) and solving the 1st order ODE leads to

$$T_b(z) = T_{in} + \frac{P_{plate}}{\dot{m}c_p}\left[\frac{\cos\left(\frac{\pi\delta}{H_e}\right) - \cos\left(\frac{\pi(z+\delta)}{H_e}\right)}{\cos\left(\frac{\pi\delta}{H_e}\right) - \cos\left(\frac{\pi(H+\delta)}{H_e}\right)}\right] \tag{35}$$

Thus, for a set of data specific to the UMLRR (P_{plate}, H, W, δ, $\dot{m}$, T_{in}, etc. -- see below for specific values), eqn. (35) gives the desired axial bulk coolant temperature profile.

The Heat Transfer Coefficient

Even with a known axial profile for the coolant temperature, one still needs a reasonable estimate of the heat transfer coefficient, h, to compute the plate surface temperature profile, $T_c(z)$. This parameter, however, is usually obtained from empirical correlations that are given in terms of the local fluid properties, the type of flow, and the geometry of the system. There are a variety of these heat transfer correlations available in the literature for a wide range of situations. These correlations can vary significantly depending upon the flow regime that is present (i.e. laminar or turbulent flow) and whether the flow is developing or fully developed. Note also that, even for fully developed flow, the heat transfer coefficient may be a function of position, $h \rightarrow h(z)$, since the correlations are often evaluated using the local bulk fluid properties. Thus, if the variation of $T_b(z)$ is significant, the variation in the fluid properties may also be important.

Before specifying particular correlations for h, we first define a number of dimensionless parameters that are often used within the empirical correlations:

$$\text{Nusselt Number} \qquad Nu = \frac{hD_h}{k} \tag{36}$$

Reynolds Number $$Re = \frac{\rho V D_w}{\mu} \quad (37)$$

Prandtl Number $$Pr = \frac{\mu c_p}{k} \quad (38)$$

where

Heated Diameter $$D_h = \frac{4 \text{ x flow area}}{\text{heated perimeter}} = \frac{4A_f}{P_h} \quad (39)$$

Wetted Diameter $$D_w = \frac{4 \text{ x flow area}}{\text{wetted perimeter}} = \frac{4A_f}{P_w} \quad (40)$$

Mass Flow Rate $$\dot{m} = \rho A_f V \quad (41)$$

where the average fluid velocity is given by the symbol V, and ρ, μ, k, and c_p are the standard symbols for the density, viscosity, thermal conductivity, and specific heat of the fluid, respectively. Note that the wetted diameter is usually referred to as the hydraulic diameter (usually with the symbol D_h).

Now, for **internal single-phase fully-developed turbulent flows**, the Dittus Boelter correlation is often used to estimate an appropriate convective heat transfer coefficient, where

$$Nu = 0.023\, Re^{0.8}\, Pr^n \quad (42)$$

with n = 0.3 when the fluid of interest is being cooled, and n = 0.4 when the fluid is being heated. Note also that all the fluid properties that go into the computation of Re and Pr for use in eqn. (42) are evaluated at the local bulk fluid temperature, $T_b(z)$. Note that, in the literature, this relationship is recommended for use for situations where $Re \geq 10{,}000$ and $0.7 \leq Pr \leq 160$.

An alternative expression for the Nusselt number for turbulent flow applications, developed by Sieder and Tate, that addresses the difference between the viscosity of the bulk coolant and that of the coolant adjacent to the clad wall (since the temperatures and viscosities at these locations can be quite different) is given as

$$Nu = 0.027\, Re^{0.8}\, Pr^{1/3} \left(\frac{\mu}{\mu_s} \right)^{0.14} \quad (43)$$

Here, the subscript s refers to the surface of the cladding. Thus, all properties should be evaluated at the bulk coolant temperature except for μ_s, which should be evaluated at the clad surface temperature. Both correlations, the Dittus Boelter and Sieder Tate relationships, are discussed in further detail in **Fundamentals of Heat and Mass Transfer** by F. P. Incropera and D. P. DeWitt. Note that, if the Sieder Tate correlation is used, an iterative scheme is needed to converge on the correct value of the surface temperature and the value of μ_s. Since the Dittus Boelter relation uses properties evaluated at only the bulk fluid temperature, no iteration is required for this correlation.

For **single phase fully-developed laminar flow** problems, where Re ≤ 2300, the combined fluid flow and heat transfer problem can be solved analytically for certain relatively simple situations. In particular, for a constant wall heat flux or a constant wall temperature, one can simply "look up" the analytical solution. Unfortunately, however, the problem of interest here has neither a constant heat flux nor a constant wall temperature. To resolve this situation, one often assumes that the real result lies between these two situations -- and, lacking further information, an average value of the analytically-derived Nusselt number is often used. We will take this approach here and use the analytical relations given in Table 8.1 from **Fundamentals of Heat and Mass Transfer** by F. P. Incropera and D. P. DeWitt (see below). Thus, for internal laminar flow problems, Nu = constant, where the constant can be obtained from averaging the values in the given table for the geometry of interest.

TABLE 8.1 Nusselt numbers and friction factors for fully developed laminar flow in tubes of differing cross section

Cross Section	$\frac{b}{a}$	$Nu_D \equiv \frac{hD_h}{k}$ (Uniform q_s'')	$Nu_D \equiv \frac{hD_h}{k}$ (Uniform T_s)	$f\,Re_{D_h}$
	—	4.36	3.66	64
	1.0	3.61	2.98	57
	1.43	3.73	3.08	59
	2.0	4.12	3.39	62
	3.0	4.79	3.96	69
	4.0	5.33	4.44	73
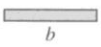	8.0	6.49	5.60	82
	∞	8.23	7.54	96
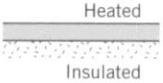 Heated / Insulated	∞	5.39	4.86	96
	—	3.11	2.47	53

Used with permission from W. M. Kays and M. E. Crawford, *Convection Heat and Mass Transfer*, McGraw-Hill, New York, 1980.

Note that there is a transition region between laminar and turbulent flow where the above correlations are not fully valid. However, for the current study, we will use the above table for flows with Re ≤ 2300 (laminar region) and use either eqn. (42) or eqn. (43) for all cases where Re ≥ 2300 (transition and turbulent regions). In addition, we will also ignore entrance effects altogether and simply apply these expressions for fully developed flow along the full length of the fuel assembly.

Thus, given information about the fluid environments (flow parameters, bulk temperatures, and material properties evaluated at these temperatures), we can use the above information to estimate the Nusselt number at any point along the channel height. With Nu known, eqn. (36) gives the desired heat transfer coefficient, h(z), which can then be used in eqn. (15a) [or eqn. (30)] to compute the axial profile of the plate's surface temperature.

Water Properties versus Temperature

The properties of liquid water at atmospheric pressure are available from several sources (i.e., see Perry's Chemical Engineer's Handbook (1999) or browse the web at www.thermexcel.com). A polynomial curve fit was performed to the data and the following equations can be used to evaluate the physical properties of liquid water at atmospheric pressure as a function temperature:

$$\mu(T) = 3.118\times10^{-11}T^4 - 8.702\times10^{-9}T^3 + 9.531\times10^{-7}T^2 - 5.427\times10^{-5}T + 1.772\times10^{-3} \qquad (44)$$

$$\rho(T) = 1.583\times10^{-5}T^3 - 5.947\times10^{-3}T^2 + 1.718\times10^{-2}T + 1000 \qquad (45)$$

$$c_p(T) = 3.149\times10^{-6}T^4 - 7.683\times10^{-4}T^3 + 7.403\times10^{-2}T^2 - 2.851T + 4215 \qquad (46)$$

$$k(T) = -7.310\times10^{-6}T^2 + 1.840\times10^{-3}T + 0.5695 \qquad (47)$$

In these equations, temperature (T) has units of °C, dynamic viscosity (μ) has units of kg/m-s, density (ρ) has units of kg/m^3, specific heat (c_p) is given in units of J/kg-K, and the thermal conductivity (k) has units of W/m-K. These functions are especially useful in computer calculations. In the current mathematical model, eqns. (44) – (47) are used, as needed, to evaluate the viscosity, density, specific heat, and thermal conductivity of water as a function of water temperature.

Additional Considerations for the Natural Convection Case

At this point we have a complete model for determining the desired axial temperature profiles within the coolant channels in the UMLRR assuming, of course, that all the pertinent design and operational data for the system are available -- including the channel mass flow rate. In the forced flow mode, the channel mass flow rate, $\dot{m}$, can be determined from the overall pump flow rate and the flow distribution in the various in-core elements (this is a quantity that we know and it is independent from the operating power level). In natural convection flow, however, things are a bit more complicated, since the channel mass flow rate is directly related to the temperature (and density) differences between the channel and the surrounding pool. Thus, for this case, $\dot{m}$ is a strong function of the average channel temperature and the buoyancy forces that result from the fluid density differences. This makes eqn. (28) nonlinear and much more difficult to solve -- and, to make matters worse, we can't even write a closed form expression for the actual functional relationship, $\dot{m} = f(T_b)$, that is involved here.

However, we do understand the fundamental physics that is associated with natural convection, so we can formulate an algorithm for including density effects into the above model. In particular, consider the sketch given in Fig. 7. This diagram shows two channels, a coolant channel and a much larger pool channel, that are connected by a common plenum at the top and bottom. Each plenum region has a common pressure denoted as P_{top} and P_{bot}, for the upper and lower regions, respectively. In the large pool channel, the flow is downward, but the actual fluid

velocity here is very low (because of the large flow area). In the coolant channel within the core region, the flow is upward, with a much larger fluid velocity relative to the pool velocity (because of the much smaller flow area). Flow in these channels can be approximated by the general energy equation for "quasi" steady-state incompressible flow (see any standard fluid mechanics text):

$$\frac{P_1}{\gamma}+\alpha_1\frac{v_1^2}{2g}+z_1-h_L=\frac{P_2}{\gamma}+\alpha_2\frac{v_2^2}{2g}+z_2 \qquad (48)$$

where we have used standard notation ($\gamma=\rho g$ is the specific weight, α is the kinetic energy correction factor, etc.), with h_L representing the head loss due to friction in the system. In this equation, point 1 represents the channel inlet and point 2 the channel outlet (the energy equation is always written in the direction of flow).

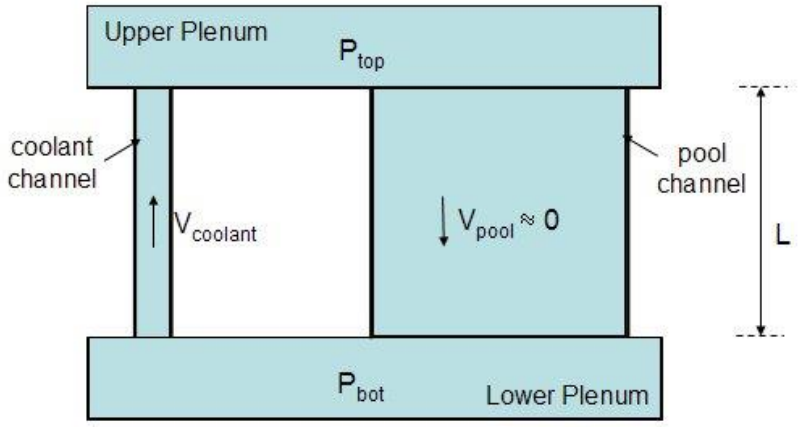

Fig. 7 Free convection path completed by the common upper and lower plenum regions.

Writing this equation specifically for the "pool channel" where the velocity is essentially zero and there are no friction losses gives

$$\frac{P_2}{\gamma_{pool}}-\frac{P_1}{\gamma_{pool}}=\frac{\Delta P}{\rho g|_{pool}}=z_1-z_2$$

or, $$\Delta P=P_{bot}-P_{top}=\rho_{pool}gL \qquad (49)$$

where L is the full length of the channel (note that $L \geq H$). This relationship is exactly what was expected from our understanding of fluid statics -- where the increase in pressure in a near static fluid column of height L is simply due to the weight of the fluid in the column.

Now, writing the energy equation in the direction of flow for the "coolant channel" where the flow is in the upward direction, gives

$$\frac{P_1}{\gamma_{coolant}}-\frac{P_2}{\gamma_{coolant}}=\frac{\Delta P}{\rho g|_{coolant}}=z_2-z_1+h_L$$

or, $$\Delta P=P_{bot}-P_{top}=\rho_{coolant}gL+\rho_{coolant}gh_L \qquad (50)$$

In developing eqn. (50), we have cancelled the kinetic energy terms since the velocities at the inlet and outlet of the channel are essentially the same, and we have assumed that the density change is relatively small so that an average (constant) density can be used in the energy equation (that is, $\rho_{bot} \approx \rho_{top} = \rho_{coolant} = \rho_{b_{ave}}$).

Since the top and bottom of the pool and coolant channels have a common upper and lower plenum region, the ΔP in eqns. (49) and (50) must be the same. Thus, equating these expressions gives

$$\Delta P_{bouyancy} = \left(\rho_{pool} - \rho_{coolant}\right) gL = \Delta\rho gL = \rho_{coolant} gh_L = \Delta P_{friction} \tag{51}$$

The first three expressions in this equation are related to the buoyancy force that is developed due the density difference in the pool and the coolant channels, and the last two terms are due to the friction losses along the coolant channel. In words, it simply says that, in steady-state, the ΔP caused by the buoyancy forces must be identical to the ΔP due to friction -- that is, the velocity that develops in the channel in natural convection flow will increase until the friction loss in the channel exactly balances the buoyant forces on the channel. With this understanding, we now have a way to relate the temperature of the channel fluid to the mass flow rate within the channel!

In particular, for viscous internal flow problems, the friction loss in a channel of constant area is given by

$$h_L = f\frac{L}{D_h}\frac{V^2}{2g} + \left(\sum_i K_i\right)\frac{V^2}{2g} \tag{52}$$

where D_h is the hydraulic diameter, L is the length of the channel, f is the dimensionless Darcy friction factor, K_i is the loss coefficient associated with the i^{th} "minor loss" component within the system (accounts for entrance and exit losses), and V is the channel average velocity.

For **laminar flow** situations, the friction factor, f, is given by

$$f = \frac{C}{Re} \qquad \text{(laminar flow)} \tag{53}$$

where C is given for several different channel geometries in Table 8.1 from **Fundamentals of Heat and Mass Transfer** by F. P. Incropera and D. P. DeWitt (see above) and, for **turbulent flows** in smooth channels, it can be approximated with reasonable accuracy with the Blasius equation,

$$f = \frac{0.3164}{Re^{0.25}} \qquad \text{(turbulent flow in a smooth channel)} \tag{54}$$

Well, the above development essentially completes the model for the case of natural convection flow. Since we cannot write a simple explicit expression for $\dot{m} = f(T_b)$, we will need to implement the model using an iterative scheme, as follows:

1. Guess a channel mass flow rate, $\dot{m}$.
2. With $\dot{m}$ known, compute an average value for the channel coolant temperature, where

$$T_{b_{ave}} = \frac{1}{H}\int_0^H T_b(z)dz \tag{55}$$

and using $T_b(z)$ from eqn. (35), we have

$$T_{b_{ave}} = T_{in} + \frac{P_{plate}}{\dot{m}c_p}\left[\frac{\cos\left(\frac{\pi\delta}{H_e}\right) + \frac{H_e}{\pi H}\sin\left(\frac{\pi\delta}{H_e}\right) - \frac{H_e}{\pi H}\sin\left(\frac{\pi(H+\delta)}{H_e}\right)}{\cos\left(\frac{\pi\delta}{H_e}\right) - \cos\left(\frac{\pi(H+\delta)}{H_e}\right)}\right] \tag{56}$$

3. Using this average temperature and the pool temperature, compute the average fluid densities in the channel and pool via eqn. (45) and the average change in fluid density using

$$\Delta\rho = \rho_{pool} - \rho_{b_{ave}} = \rho(T_{pool}) - \rho(T_{b_{ave}}) \tag{57}$$

4. Now, using eqns. (51)-(54) and the above supporting discussion, as appropriate, compute the average velocity in the coolant channel and a new mass flow rate based on this average velocity.

5. Compare the mass flow rate guess from Step #1 and the computed $\dot{m}$ from Step #4. If these agree within some specified tolerance, then the iterative scheme is complete, the correct $\dot{m}$ that balances the buoyancy forces and friction forces is known, and $T_b(z)$ can be computed from eqn. (35) (using the same approach as for forced flow with known $\dot{m}$). At this point, one can continue with any additional analyses that may be needed.

   If, however, the two mass flow rates differ by an amount greater than the desired accuracy, then the iterative scheme has not yet converged, and one must make another guess for $\dot{m}$ and go back to Step #1. Note that there are a number of options here for automating the next guess for $\dot{m}$. For example, if we denote k as the iteration counter, then one option is simply to define the guess for iteration k+1 as the computed value of $\dot{m}$ for the current step (i.e. for iteration k).

UMLRR Operational **and Design Data**

The above development presents a mathematical model for finding the axial profiles for the coolant and plate surface temperatures within a standard fuel element in the UMass-Lowell research reactor (UMLRR). The model accounts for both forced and natural convection flows, with the nonlinear nature of the natural convection model requiring an iterative solution algorithm. The model development given here is applicable to any plate-type fuel assembly with a number of parallel plates and an axial power profile that can be approximated as a simple chopped sinusoid. Our current interest, of course, is the application of this mathematical model to the UMLRR and a set of UMLRR-specific operational and design data are included below to support the implementation of the theoretical development. These data can be used along with the above model to obtain explicit results (i.e., axial profiles for T_b, T_c, T_s, and T_m) for the UMLRR under a variety of operational conditions.

UMLRR Plate and Channel Geometry Information (also see Fig. 4):

a = 0.0255 cm	half thickness of uranium silicide fuel meat (0.0510/2 cm)
b = 0.038 cm	thickness of aluminum clad
w = 6.085 cm	width of fuel meat
W = 6.604 cm	width of channel
H = 59.69 cm	active fuel height
L = 63.5 cm	length of coolant channel
D = 2c = 0.2963 cm	thickness of coolant channel
δ = 6 cm	estimate of axial reflector savings
N_{fp} = 320	number of fuel plates (20 assemblies × 16 plates per element)
N_{ch} = 378	# of coolant channels (21 assemblies × 18 channels per element)

Material Properties (water properties vs temperature are already given in above discussion)

k_{fuel} = 15 W/m-K	thermal conductivity of U_3Si_2-Al uranium silicide fuel
k_{clad} = 180 W/m-K	thermal conductivity of aluminum clad

Operational Data:

$T_{pool} = T_{in}$ = variable — pool and core inlet temperature (nominal value is about 20 C)

$K = 0.5 + \alpha$ — loss coefficients (sum of channel entrance and exit losses)

$$\alpha = \begin{cases} 2.0 & \text{laminar flow} \\ 1.05 & \text{turbulent flow} \end{cases}$$ kinetic energy correction factors

$$F_R = \begin{cases} 1.0 & \text{average plate} \\ 1.45 & \text{hot plate} \end{cases}$$ radial peaking factors (adjusts average plate power)

P_{tot} = variable — reactor power (up to 1 MW/100 kW in forced/free flow mode)

$$\dot{m} = \begin{cases} f(Q_{core}) & \text{forced flow} \\ f(T_{b_{ave}}) & \text{free convection} \end{cases}$$ channel mass flow rate

Notes:

1. For forced flow mode, the mass flow rate per channel is computed based on the total core volumetric flow rate, Q_{core} (nominal value of about 1650 gpm). Previous work has shown that the current core configuration has about 72% of the total flow going through the fuel elements and, with N_{ch} channels, the volume flow rate per channel is $Q_{ch} = 0.72*Q_{core}/N_{ch}$. Then, the mass flow rate per channel is simply $\dot{m} = \rho Q_{ch}$.

2. In natural convection mode, the channel mass flow rate is an implicit function of the channel average coolant temperature -- and this relationship has already been described in detail in the above development.

3. The M-2-5 core arrangement has 21 total fuel assemblies -- 19 full fuel elements and 2 partial fuel assemblies. A partial assembly has the same physical appearance and dimensions as a full assembly, but each plate has half the fuel meat thickness (but the overall plate thickness is unchanged). For the computation of the average power per plate, we use 20 equivalent full fuel assemblies with 16 fuel plates per assembly. However, to determine the coolant flow rate per channel, we use 21 assemblies times 18 channels per element (17 full interior channels between 18 plates and two half channels on the ends).
4. Finally, since the methodology developed here assumes 1-D energy flow from the fuel to the coolant, the actual fuel meat thickness, w, is not used explicitly -- instead, the full channel width, W, is used to compute both the average heat flux and the fluid flow area. In contrast, the actual active fuel height, H, is used for representing the axial power profile, and the channel length, L, is used to compute the friction loss in the channel for the natural convection cases.

Typical Results

A Matlab program, **sstemp_umlrr**, was written to implement the above mathematical model, and a graphical user interface was created to allow the user to easily explore a number of variations (variable power level, flow rate in forced convection mode, inlet temperature, etc.). The Matlab GUI is called **sstemp_umlrr_gui** and a sample screen of the actual graphical user interface is shown in Fig. 8. This specific screen shows a 200 kW natural convection case for the hot channel with a built-in radial peaking factor of 1.45 (note that a core power level of 200 kW is above the current licensed limit for natural convection operation of the UMLRR), where the available user options are given in the upper left portion of the screen, and the graphical and tabular results for the particular run are given in the right and lower left portions of the screen, respectively.

Concerning a description/explanation of the code results, here we only briefly discuss the resultant axial temperature profiles for two nominal cases:

Case 1: Forced flow, average plate analysis, P_{core} = 1000 kW, Q_{core} = 1650 gpm, T_{in} = 20 C, Sieder Tate correlation.

Case 2: Natural convection, average plate analysis, P_{core} = 100 kW, T_{in} = 20 C, Sieder Tate correlation selected but not used because flow regime was laminar.

The resultant profiles from the **sstemp_umlrr** code for the two cases are shown in Figs. 9 and 10, respectively. The nominal forced flow case, as seen in Fig. 9, has sufficient cooling (due to the relatively large flow rate) so that the coolant temperature rise along the average channel is less than 4 C, and the corresponding clad and fuel temperature profiles peak somewhat on the downstream side of core center (recall that the assumed axial power profile is symmetric around center). For this situation, the clad and fuel profiles are dominated by the power distribution profile, with a slight tilt to account for the increasing bulk coolant temperature with increasing z.

For the nominal natural convection case, as shown in Fig. 10, the coolant temperature rise along the channel is significantly larger, even though the core power level is only 100 kW (as compared to the 1000 kW power for Case 1). The near 20 C increase, of course, is due to the much lower channel mass flow rate that develops in the natural convection case (due to the coolant density difference between the heated channel and the cooler pool coolant temperature). In this case, the clad and fuel temperature profiles are dominated by the axial coolant profile, and

only weakly affected by the axial power profile -- thus, for the natural convection case, the shape of all the temperature profiles are quite similar.

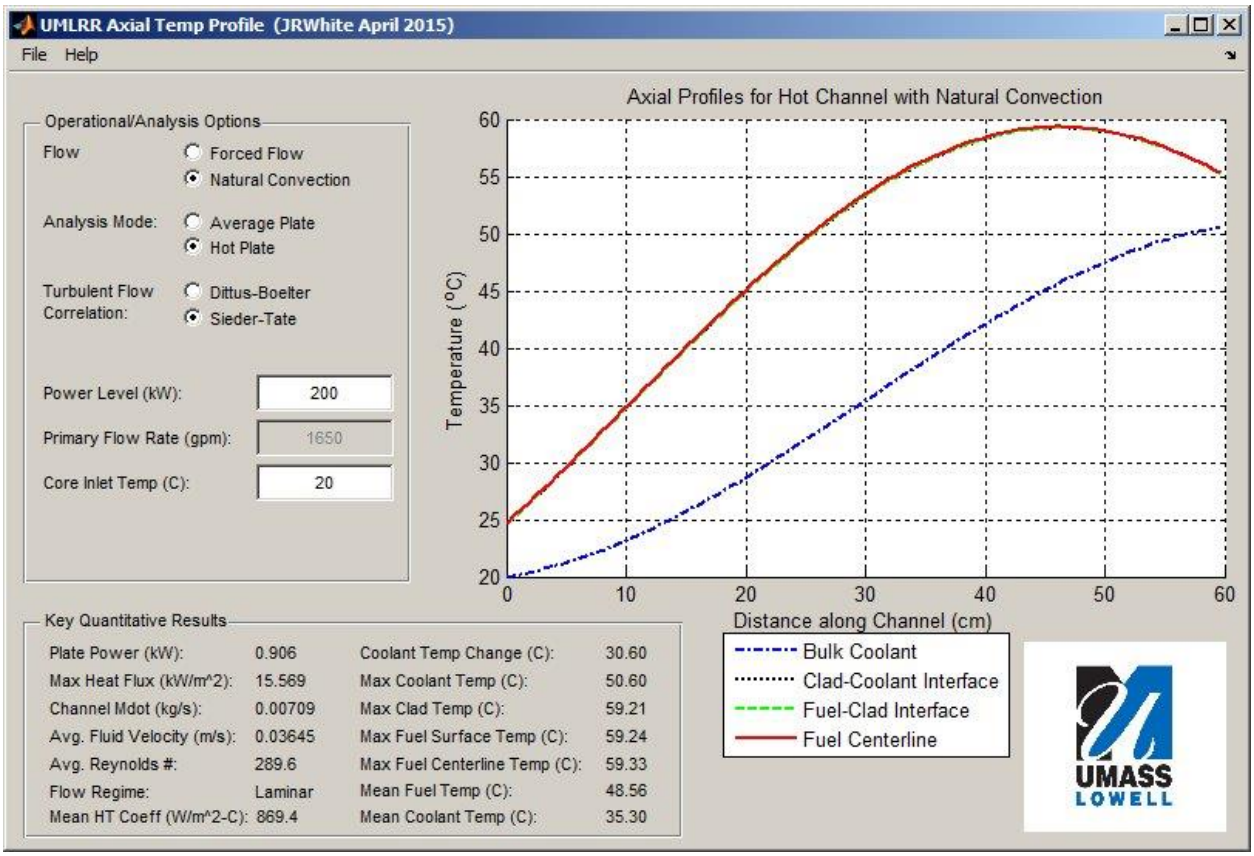

Fig. 8 Graphical user interface for the sstemp_umlrr_gui code.

Summary

Well, we have accomplished our original goal of developing an appropriate mathematical model and illustrating the typical axial temperature profiles that can be expected within the UMLRR fuel assembly geometry. This documentation and the available GUI should serve as valuable educational tools -- allowing the student the ability to explore alternate operational situations, and hopefully to obtain a good understanding of nuclear heat transport in plate-type geometries.

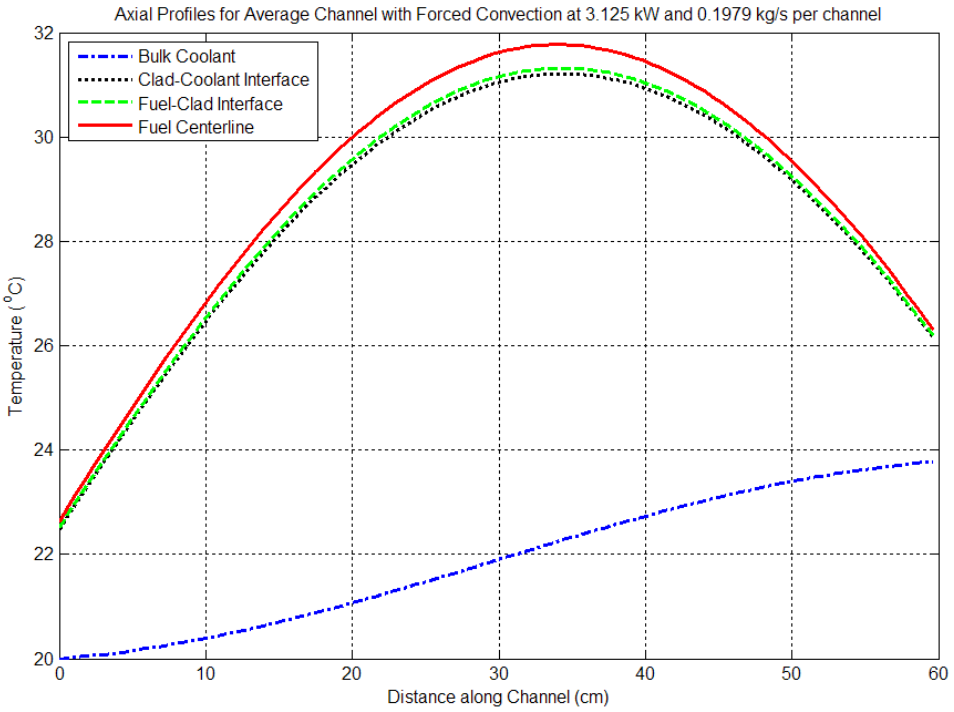

Fig. 9 Axial Temperature profiles for Case 1 (forced convection mode).

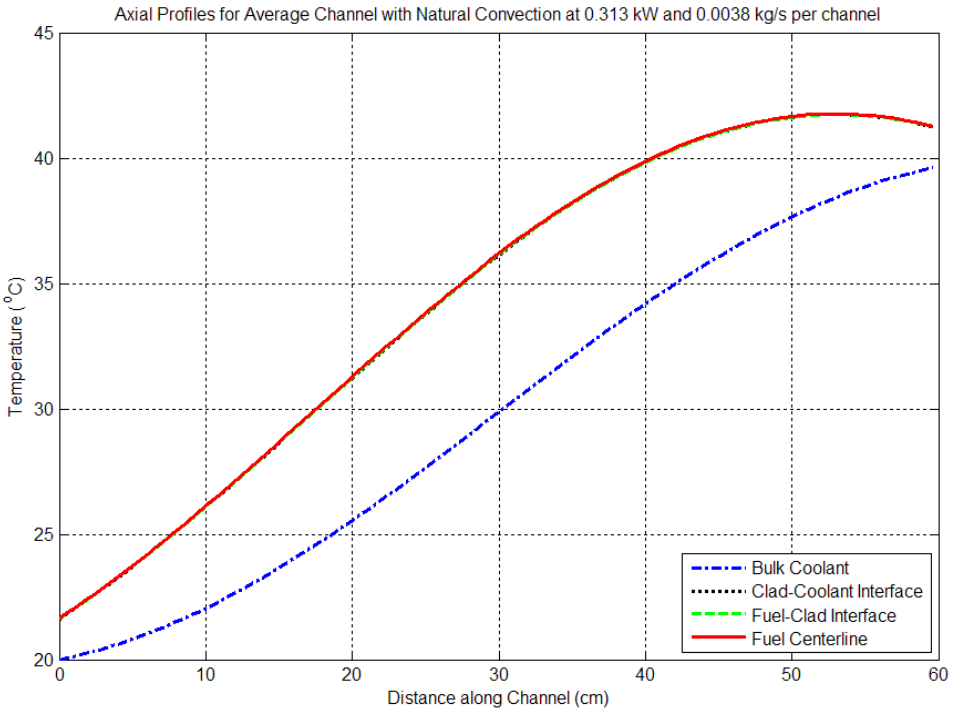

Fig. 10 Axial Temperature profiles for Case 2 (natural convection mode).